Received: 21 November 2022 | Revised: 27 April 2023 | Accepted: 10 May 2023

DOI: 10.1111/cas.15855

Cancer Science WILEY

ORIGINAL ARTICLE

Acute myeloid leukemia (AML)-derived mesenchymal stem cells induce chemoresistance and epithelial–mesenchymal transition-like program in AML through IL-6/JAK2/STAT3 signaling

Jianle Lu[1] | Qiaomei Dong[2] | Shuling Zhang[1] | Youfan Feng[1] | Jincai Yang[1] | Li Zhao[1,2,3]

[1]The First Clinical Medical College, Lanzhou University, Lanzhou, China

[2]Central Laboratory, The First Affiliated Hospital, Lanzhou University, Lanzhou, China

[3]Gansu Key Laboratory of Genetic Study of Hematopathy, Lanzhou, China

Correspondence
Li Zhao, Central Laboratory, The First Affiliated Hospital, Lanzhou University, No. 1 Donggang West Road, Chengguan District, Lanzhou 730000, China.
Email: zhaoli@lzu.edu.cn

Funding information
Foundation of the First Hospital of Lanzhou University, Grant/Award Number: ldyyyn2020-105 and ldyyyn2020-60; Fundamental Research Funds of Lanzhou University, Grant/Award Number: lzujbky-2021-kb39; Interdisciplinary Project of the First Hospital of Lanzhou University, Grant/Award Number: ldyyyn2020-89

Abstract

Acute myeloid leukemia (AML) has a high rate of treatment failure due to increased prevalence of therapy resistance. Mesenchymal stem cells (MSCs) in the leukemia microenvironment contribute to chemoresistance in AML, but the specific mechanism remains unclear. The critical role of the epithelial–mesenchymal transition (EMT)-like profile in AML chemoresistance has been gradually recognized. However, there is no research to suggest that the AML-derived bone marrow mesenchymal stem cells (AML-MSCs) induce the EMT program in AML thus far. We isolated AML-MSCs and cocultured them with AML cells. We found that AML-MSCs induced a significant mesenchymal-like morphology in drug-resistant AML cells, but it was scarce in parental AML cells. The AML-MSCs promoted growth of AML cells in the presence or absence of chemotherapeutics in vitro and in vivo. Acute myeloid leukemia MSCs also induced EMT marker expression in AML cells, especially in chemoresistant AML cells. Mechanistically, AML-MSCs secreted abundant interleukin-6 (IL-6) and upregulated IL-6 expression in AML cells. Acute myeloid leukemia cells upregulated IL-6 expression in AML-MSCs in turn. Meanwhile, AML-MSCs activated the JAK2/STAT3 pathway in AML cells. Two JAK/STAT pathway inhibitors counteracted the AML-MSCs induced morphology change and EMT marker expression in AML cells. In conclusion, AML-MSCs not only promote the emergence of chemoresistance but also enhance it once AML acquires chemoresistance. AML-MSCs induce EMT-like features in AML cells; this phenotypic change could be related to chemoresistance progression. AML-MSCs induce the EMT-like program in AML cells through IL-6/JAK2/STAT3 signaling, which provides a therapeutic target to reverse chemoresistance in AML.

Abbreviations: AML, acute myeloid leukemia; AML-MSC, AML bone marrow-derived MSC; EMT, epithelial mesenchymal transition; HMSC, healthy bone marrow-derived MSC; IL-6, interleukin 6; MSC, mesenchymal stem cell; STAT3, signal transducer and activator of transcription 3.

Jianle Lu and Qiaomei Dong contributed equally.

KEYWORDS
acute myeloid leukemia, chemoresistance, epithelial–mesenchymal transition, IL-6, mesenchymal stem cell

1 | INTRODUCTION

Acute myeloid leukemia is a highly heterogeneous hematopoietic disorder that develops due to immature myeloid cells' accumulation and clonal expansion. Although the treatment of AML has been continuously developed in recent years, the prognosis of most patients is still poor due to the occurrence of drug resistance. Approximately 50% of patients develop resistance during chemotherapy, leading to disease progression and relapse. Several mechanisms of drug resistance in AML have been identified. However, clinical trials of treatments targeting these mechanisms have been unsuccessful.[1,2] In recent years, it has been known that the bone marrow microenvironment plays a critical role in AML progression. Studies have shown that interactions between MSCs and AML cells promote chemoresistance and disease relapse, but the underlying mechanisms remain to be understood.[3,4]

Mesenchymal stem cells are multipotent progenitor cells that can differentiate into osteocytes, adipocytes, and chondrocytes. Mesenchymal stem cells are present in various normal tissues, including bone marrow, adipose, and umbilical cord. They can also be isolated from tumor tissues. It has been reported that AML-MSCs enable the abilities of multiple lineage differentiation, rapid cell proliferation, self-renewal, and release of high amounts of cytokines and growth factors.[5] De novo AML-MSCs display a significant increase in the expression levels of vascular endothelial growth factor (VEGF), stromal cell-derived factor 1 (CXCL-12), Receptor of prostaglandin E2 (RPGE-2), indoleamine 2,3-dioxygenase, IL-1β, IL-6, and IL-32 compared to HMSCs.[6] Multiple cytokines, especially IL-6 and IL-8, have been shown to support chemoresistance in AML.[7,8]

Epithelial–mesenchymal transition refers to a reversible process in which cancer cells become migratory and invasive mesenchymal-like cells while acquiring cancer stem cell properties and therapy resistance. Epithelial–mesenchymal transition is regulated by several cytokines and signaling pathways, which can activate the Snail, Twist1, and Zeb families of EMT transcription factors. Epithelial–mesenchymal transition transcription factors can then bind to the promoter region of EMT-related genes, regulating the expression of E-cadherin, N-cadherin, and vimentin.[9] Epithelial–mesenchymal transition mediates chemoresistance in lung cancer,[10] prostate cancer,[11] colon cancer,[12] breast cancer,[13] and others. Moreover, the interaction between tumor cells and other cells that compose the tumor microenvironment triggers EMT in cancer,[14] and MSCs can promote the EMT of tumor cells through secreted cytokines.[15] The EMT program has been mainly studied in epithelial tumors but less in nonepithelial neoplasms. In recent years, relevant studies have shown that EMT also plays an essential role in hematological malignancies.[16–18] Epithelial–mesenchymal transition transcription factors participate in hematopoiesis and leukemogenesis, and their abnormal expressions render leukemia cells resistant to therapy. Twist1, Snail1, and vimentin are all highly expressed in leukemia patients and associated with chemoresistance.[19–21] Under hypoxia, hypoxia-inducible factor-1α can activate EMT in leukemia stem cells, increasing the resistance of AML cells to cytarabine.[22] MicroRNA-130a can increase AML cell chemoresistance by EMT.[23] However, no attention has been paid to the potential of the AML-MSC-induced EMT program in AML.

In this study, we isolated AML-MSCs and cocultured AML cells with AML-MSCs in direct or indirect contact ways. The NOD-SCID mouse xenograft model was also used to assess the effects of AML-MSCs on AML growth in vivo. In another way, we were interested in exploring what role the AML-MSCs played when chemoresistance emerged. Therefore, we cocultured chemoresistant AML cells with AML-MSCs in the same way. We investigated the effects of AML-MSCs on AML proliferation and chemoresistance in vitro and in vivo; the underlying mechanism was also explored.

2 | MATERIALS AND METHODS

2.1 | Isolation of AML-MSCs

We obtained bone marrow aspirates from newly diagnosed AML patients in the First Hospital of Lanzhou University. Written informed consent was obtained from patients or their legal guardians. All procedures were authorized by the Institutional Ethics Committee of the First Hospital of Lanzhou University and carried out according to the Declaration of Helsinki. The acquired fresh bone marrow aspirates were quickly plated in DMEM/F12 containing 10% FBS (Excell Bio) and 1% penicillin/streptomycin. The culture medium was renewed every 2 days after seeding. We used PBS to wash the culture flask to remove the suspension cells and cell debris. The AML-MSCs adhered tightly to the flask wall, were digested with 0.25% trypsin, and expanded when cell confluence reached 80%. P3-P6 of AML-MSCs were used in the following experiments.

2.2 | Induced differentiation of MSCs

For osteogenic differentiation, MSCs were plated in 6-well plates, and osteogenic induction medium (Fuyuan Bio) was added according to the manufacturer's instructions when cell confluence reached approximately 60%. After 21 days of differentiation, the cells were fixed with 4% paraformaldehyde and stained with Alizarin Red. For adipogenic differentiation, MSCs were cultured in adipogenic induction medium (Fuyuan Bio) after confluency reached 90%. After 4 days of differentiation, cells were fixed with 4% paraformaldehyde and stained with Oil Red O. For chondrogenic differentiation,

approximately 1×10^6 MSCs were seeded in the centrifugal tube and cultured in the chondrogenic induction medium (Fuyuan Bio) as recommended by the manufacturer. After 20 days of differentiation, the formed cell cluster was fixed with 4% paraformaldehyde and sliced, and finally stained with Alcian Blue solutions.

2.3 | Flow cytometric analysis

Flow cytometry was carried out to confirm the surface markers of AML-MSCs or HMSCs. The MSCs (1×10^6) were prepared and incubated with anti-29, anti-CD34, anti-CD45 (all purchased from BioLegend), and anti-CD44 Abs (Multisciences), then submitted to flow cytometric analysis (BD). The data analysis was undertaken using FlowJo software.

2.4 | Cell lines and cocultures

The human adriamycin-resistant AML cell line K562-ADM, the parental cell line K562, and HMSCs were obtained from the Central Laboratory of the First Hospital of Lanzhou University. The human HL60 cell line was purchased from the Otwo Biotech , and the human adriamycin-resistant AML line, HL60-ADR cell line, was purchased from Winter Biotechnology . These cell lines were grown in RPMI-1640 or DMEM/F12 supplied with 10% FBS at 37°C in a humid atmosphere containing 5% CO_2. In the direct-contact coculture system, 2×10^4 AML-MSCs or HMSCs were seeded in 6-well plates; 1×10^5AML cells were added when MSCs reached approximately 70% confluence. We observed the morphology and took photomicrographs of AML cells in the coculture group through the inverted biological microscope CKX41 (Olympus). In the indirect-contact coculture system, 0.4 μm Transwell inserts (NEST) were used, 1×10^5 AML-MSCs were seeded in the lower chamber and 5×10^5AML cells were planted in the upper chamber. After coculture, upper AML cells were collected for proliferation tests and mechanism studies.

2.5 | Cell proliferation and drug resistance assays

To analyze the effect of AML-MSCs on AML cell proliferation, AML-MSCs (1×10^4 cells/well) were first seeded in the lower chamber of Transwell plates (NEST); after 24 h, the culture medium was exchanged. For the drug resistance assay, different concentrations of adriamycin solutions (0.2 μg/mL for HL60 cells, 0.5 μg/mL for K562 cells, 20 μg/mL for HL60-ADR cells, and 25 μg/mL for K562-ADM cells) were added to the culture medium. Subsequently, AML cells (5×10^4 cells/well) were seeded in the upper chamber and separated from the AML-MSCs by a semipermeable membrane (0.4 μm pore size). All the cells were cultured in the Transwell coculture system for 72 h. Acute myeloid leukemia cells were collected for viability testing. Cell viability was measured by the CCK-8 Cell Counting Kit (Beyotime) according to the manufacturer's instructions; each sample was allocated in 96-well plates, and CCK-8 was added. After incubation, the absorbance (optical density) at 450 nm was measured at different time points using a multifunctional microplate reader (Thermo Fisher Scientific).

2.6 | Enzyme-linked immunosorbent assay

The IL-6 concentration in each group's supernatant was detected by a human IL-6 ELISA kit (Sino Biological) according to the manufacturer's protocol. All tests were carried out in duplicate. The IL-6 concentration (pg/mL) was defined by making a standard curve with recombinant IL-6.

2.7 | RNA extraction and real-time PCR assays

RNA was extracted with TRIzol reagent (Mei5 Biotechnology), and the RNA was reverse transcribed into cDNA using a PrimeScript RT reagent kit (Takara) according to the standard instructions. Real-time PCR was carried out using the TB Green Premix Ex Taq II kit (Takara) and detected by Roche LightCycler 480 (Roche Diagnostics). The PCR amplification was carried out according to instructions. β-Actin was used as the housekeeping gene. The sequences of the primers used were as follows: β-actin forward, 5′-TGGCACCCAGCAC AATGAA-3′ and reverse, 5′-CTAAGTCATAGTCCGCC TAGAAGCA-3′; Snail1 forward, 5′-GAGGCGGTGGCAGACTAGAGT-3′ and reverse, 5′-CGGGCCCCCAG AATAGTTC-3′; Twist1 forward, 5′-GCCAGGTACATCGACTTCCTCT-3′ and reverse, 5′-TCCATCCT CCAGACCGAGAAG-3′; vimentin forward, 5′-AGTCCACTGAGTACCGGAGAC-3′ and reverse, 5′-CATTT CACGCATCTGGCGTTC-3′; Jak2 forward 5′-ATGTCTTACCTCTTT GCTCAGTGGC-3′ and reverse, 5′-GGTTTGATCGTTTTCTTTGGC TAT-3′; Stat3 forward, 5′-GCTTCTCCTTCTGGGTCTGGC-3′ and reverse, 5′-CCTCCTT CTTTGCTGC TTTCACT-3′; and IL-6 forward, 5′-AACCTGAACCTTCCAAAGATGG-3′ and reverse, 5′-TCTGGCTTGTT CCTCACTACT-3′. The relative quantification of genes was undertaken using the $2^{-\Delta\Delta C_t}$ method.

2.8 | Protein extraction and western blot analysis

Collected cells were washed twice with ice-cold PBS, lysed using RIPA buffer (Beyotime) containing proteinase inhibitors (Beyotime) and protein phosphatase inhibitor complex (Beyotime) for 30 min at 4°C. After centrifuging at 14,000 *g* for 15 min, the supernatant was collected as protein extracts. Protein concentration was determined by a BCA kit (Solarbio). Protein (15–20 μg) was separated by 10% SDS-PAGE gels (NCM Biotechnology) and transferred onto PVDF membranes (Merck Millipore). The membranes were blocked with 5% skimmed milk powder and incubated with primary Abs at 4°C overnight. The primary Abs were Snail1 (1:1000; Cell Signaling Technology), Twist1 (1:1000; Santa Cruz Biotechnology), vimentin (1:1000; Cell Signaling Technology), Jak2 (1:1500; Huabio), Phospho-jak2 (Y1007+Y1008)

(1:1500; Huabio), Stat3 (1:1500; Huabio), Phospho-stat3 (Tyr705) (1:1500; Huabio), and β-actin (1:1000; Beyotime). β-Actin was used as the loading control. Peroxidase-conjugated secondary Ab (1:5000; Immunoway) was used to incubate the membrane at room temperature for 1 h. Finally, electrochemiluminescence was applied to detect the protein bands through a chemiluminescence imaging system (Amersham Imager 680).

2.9 | Immunofluorescence

AML-MSCs were seeded on sterile coverslips in 6-well plates at 4×10^4 cells/well, then 2×10^5 AML cells were added when MSCs reached approximately 70% confluence. After 48 h, cells were fixed with 4% paraformaldehyde at room temperature for 20 min, then permeabilized by 0.1% Triton X-100 for 20 min, followed by blocking in 5% BSA for 40 min. Cells were incubated with a fluorescently labeled Ab directed against vimentin (1:200; Huabio) at 4°C overnight. Nuclei were stained with 10 μg/mL DAPI solution, and staining was analyzed with a fluorescence microscope.

2.10 | Xenograft model

Four-week-old female NOD-SCID mice were obtained from GemPharmatech Co., Ltd and housed in a specific pathogen-free environment with a 12:12 h light:dark cycle and consistent temperature and humidity. After 1 week of adaptive feeding, all mice were randomly divided into four groups (each with five mice): HL60, HL60+adriamycin, HL60+AML-MSC, and HL60+AML-MSC+adriamycin. Mice in HL60 and HL60+adriamycin groups were then inoculated s.c. into groins with 5×10^6 HL60 cells and the other two groups were inoculated s.c. with 5×10^6 HL60 cells mixed with 1×10^6 AML-MSC cells. Tumor sizes were measured using a vernier caliper when tumors could be visualized. Tumor growth was evaluated by measurement of tumor volumes calculated as $V=(\text{length}\times\text{width}^2)/2$. When the mean tumor volume reached 100 mm^3, mice in the HL60+adriamycin and HL60+AML-MSC+adriamycin groups were i.p. injected with adriamycin at a dose of 1 mg/kg every day; the control groups were treated with saline. Three weeks after injection, mice were killed and tumors were dissected out and measured. All animal experiments were approved by the Ethics Committee of the First Hospital of Lanzhou University.

2.11 | Statistical analysis

All data values were analyzed by SPSS 24.0 software or GraphPad Prism 8.0 software. All results were shown as mean ± SD. Student's *t*-test was used to assess the difference between two groups. We used 2×3 repeated measures ANOVA to compare the mesenchymal-like

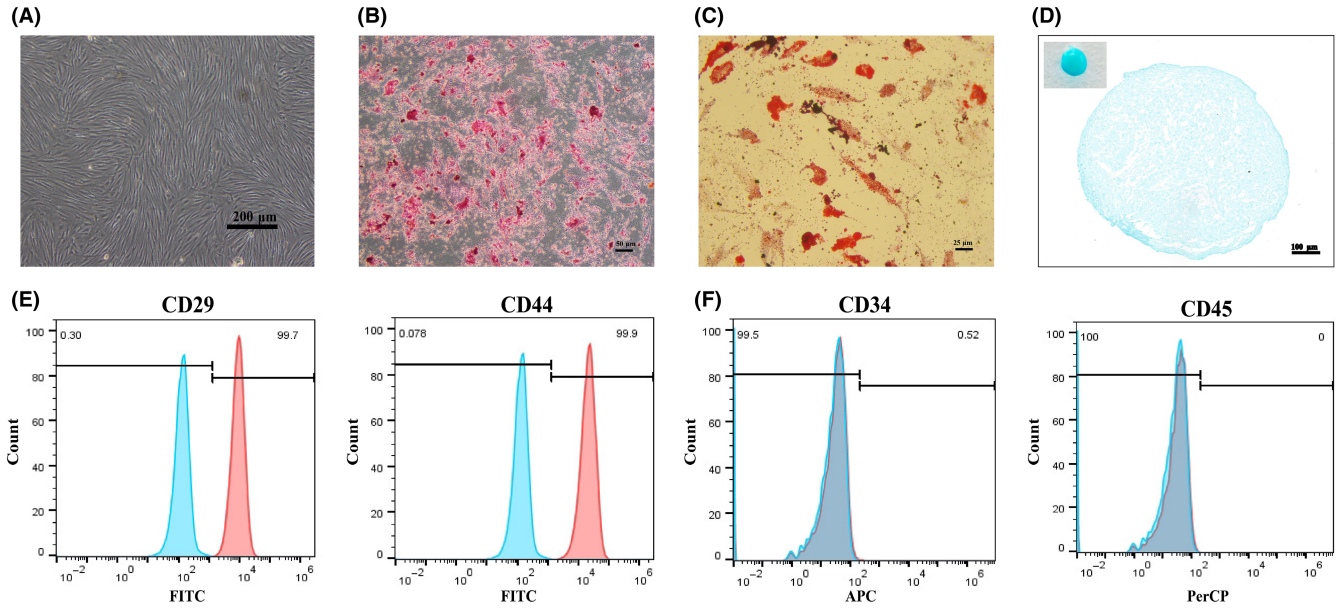

FIGURE 1 Identification of acute myeloid leukemia (AML) bone marrow-derived mesenchymal stem cells (MSCs). (A) Morphological observation of AML-MSCs in passage 2 (magnification, ×40; scale bar, 200 μm). The AML-MSCs were spindle shaped. (B) Results of Alizarin Red staining. After cultivation in osteogenic differentiation medium, AML-MSCs formed Alizarin Red-positive mineral nodes (magnification, ×100; scale bar, 50 μm). (C) Results of Oil Red O staining. After cultivation in adipogenic differentiation medium, AML-MSCs formed numerous Oil-Red-O-positive lipid droplets (magnification, ×200; scale bar, 25 μm). (D) Results of Alcian Blue staining. After cultivation in chondrogenic differentiation medium, AML-MSCs grew into a round cell cluster and were positive for Alcian Blue staining (magnification, ×8; scale bar, 100 μm). (E) Flow cytometry analysis of phenotypic markers of AML-MSCs. AML-MSCs were positive for CD29 and CD44. (F) Flow cytometry analysis of phenotypic markers of AML-MSCs. AML-MSCs were negative for CD34 and CD45. APC, allophycocyanin; FITC, fluorescein isothiocyanate; PerCP, peridinin chlorophyll A protein.

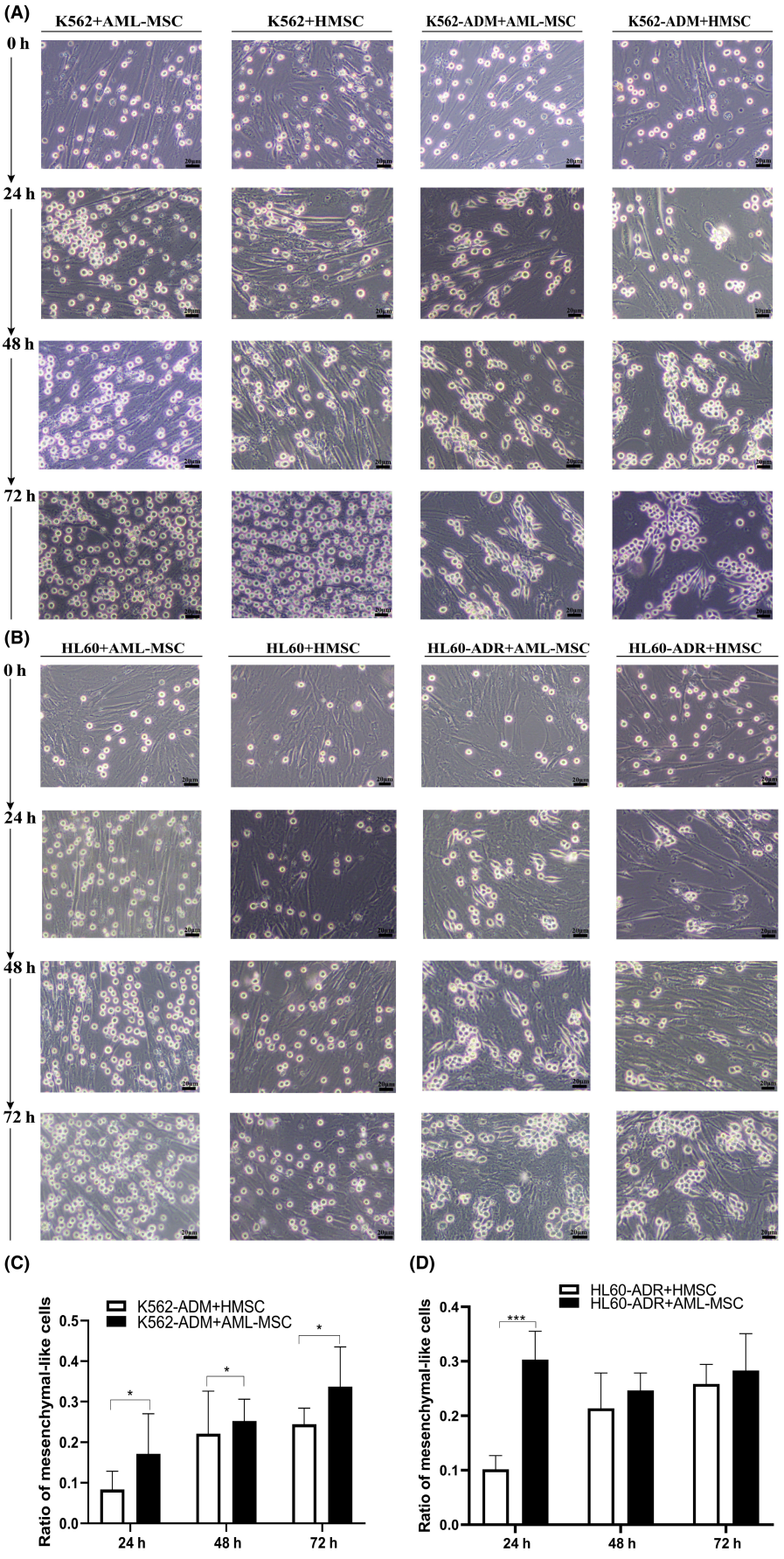

FIGURE 2 Acute myeloid leukemia (AML) bone marrow-derived mesenchymal stem cells (MSCs) significantly induce mesenchymal-like morphology in AML-resistant cells. (A) Photomicrographs of K562 and adriamycin-resistant K562-ADM cells in two coculture systems at 0, 24, 48, and 72 h (magnification, ×100; scale bar, 20 μm). (B) Photomicrographs of HL60 and adriamycin-resistant HL60-ADR cells in two coculture systems at 0, 24, 48, and 72 h (magnification, ×100; scale bar, 20 μm). (C) Quantitative analysis of mesenchymal-like K562-ADM cells in two coculture systems at 24, 48, and 72 h. (D) Quantitative analysis of mesenchymal-like HL60-ADR cells in two coculture systems at 24 h, 48 h, and 72 h. $^{*}p < 0.05$, $^{***}p < 0.001$. HMSC, healthy bone marrow-derived MSC.

AML cell numbers between two coculture groups at 24, 48, and 72 h. Differences were regarded as statistically significant when the *p* value was less than 0.05.

3 | RESULTS

3.1 | Isolation and identification of AML-MSCs

To isolate the AML-MSCs, we obtained fresh bone marrow aspirates from newly diagnosed AML patients and cultured them in specific MSC nutritional conditions. The isolated AML-MSCs were spindle in shape and adhered tightly to the wall of the culture flask in a vortex pattern (Figure 1A). To verify the multidifferentiation potential of AML-MSCs, we cultivated them in adipogenic differentiation medium, osteogenic differentiation medium, and chondrogenic differentiation medium. The AML-MSCs formed Alizarin Red-positive mineral nodes after osteogenesis induction (Figure 1B), formed numerous Oil Red O-positive lipid droplets after cultivating in adipogenic differentiation medium (Figure 1C), and formed into a round cell cluster during chondrogenic differentiation and were positive for Alcian Blue staining (Figure 1D). Therefore, it was confirmed that the isolated AML-MSCs could differentiate into osteocytes, adipocytes, and chondrocytes. Flow cytometric analysis revealed that the AML-MSCs were positive for CD29 and CD44 (Figure 1E) and negative for CD34 and CD45 (Figure 1F). These results indicated that the isolated AML-MSCs were of high purity and met the standards of the International Society of Cell Therapy for MSC identification.[24] The HMSCs were identified in the same way (Figure S1).

3.2 | Acute myeloid leukemia MSCs AML-MSC induce EMT-like program and promote adriamycin resistance of AML cells

To study the role of AML-MSCs in the progression of AML, we cocultured AML cells with AML-MSCs in a direct-contact manner for 72 h. During the coculture time, an increasing number of K562-ADM cells and HL60-ADR cells were elongated and acquired a mesenchymal-like morphology in the AML-MSCs or HMSC coculture system; the mesenchymal-like K562 and HL60 cells scarcely could be seen in the coculture systems (Figure 2A,B). To describe quantitatively this observed phenomenon, six random fields of vision were photographed through the microscope in each group; the mesenchymal-like cell counts and total cell counts in every photomicrograph were then calculated by ImageJ software (NIH). According to the calculated ratio of mesenchymal-like K562-ADM cells (Figure 2C), AML-MSCs induced many more mesenchymal-like K562-ADM cells than HMSCs ($p < 0.05$); AML-MSCs also induced much more mesenchymal-like HL60-ADR cells than HMSCs at 24 h ($p < 0.001$), as well as at 48 h and 72 h, but they were not statistically significant (Figure 2D). We thought this morphology change was closely related to chemoresistance progression. Next, we determined the effect of AML-MSCs on AML proliferation and drug sensitivity. Acute myeloid leukemia MSCs not only promoted the growth of parental and chemoresistant cells but also protected them from adriamycin-induced cell inhibition in vitro, which could also be seen in their chemoresistant cells (Figure 3A). The NOD-SCID mouse xenograft model was also used to test this effect in vivo. HL60 cells alone or mixed with AML-MSCs were transplanted s.c. into mice. Tumors developed well in the NOD-SCID mice, tumor nodules could be visualized after approximately 10 days, tumors developed faster in coculture groups, and AML-MSCs promoted the growth of HL60 cells in vivo. When tumors reached certain volumes, adriamycin treatment slowed the tumor growth in vivo, tumor volumes and weights in the coculture group treated with adriamycin were greater than HL60 group under adriamycin treatment (Figure 3B–D), indicating that AML-MSCs also promoted the chemoresistance of AML cells in vivo.

Epithelial–mesenchymal transition refers to a biological process in which tumor cells acquire mesenchymal morphology and chemoresistant phenotype. We found that AML-MSCs promoted the relative mRNA expression of EMT transcription factors: Snail and Twist1, also their downstream vimentin expression in K562 and K562-ADM cells (Figure 3E,F). Additionally, after coculture, the chemoresistant cells exhibited higher expression levels of these markers compared to the parental cells (Figure 3G). Moreover, AML-MSCs exerted similar results in HL60 and HL60-ADR cells (Figure 3H–J). Western blot assays showed that AML-MSCs upregulated Twist1 and vimentin protein expression of K562-ADM or HL60-ADR cells in the coculture system but inhibited Snail1 protein expression. There were very low expressions of Snail1, Twist1, and vimentin protein in HL60 cells and AML-MSCs had little effect on their expression. Meanwhile, AML-MSCs inhibited Snail and Twist1 expression but upregulated vimentin expression in K562 cells (Figure 3K,L). The immunofluorescence

FIGURE 3 Acute myeloid leukemia (AML) bone marrow-derived mesenchymal stem cells (MSCs) promote adriamycin resistance of AML cells and significantly induce the expression of epithelial–mesenchymal transition (EMT)-related markers in AML-resistant cells. (A) Growth rates of HL60, adriamycin-resistant HL60-ADR, K562, and adriamycin-resistant K562-ADM cells was determined by CCK-8 assay in the AML-MSC Transwell coculture system with or without adriamycin treatment. (B) Tumor images in each group. (C) Tumor weight in each group. (D) Tumor volume with time in each group. (E–G) EMT-related marker mRNA expression in K562 or K562-ADM cells were determined by PCR. (H–J) EMT-related marker mRNA expression in HL60 or HL60-ADR cells was determined by PCR. (K, L) Western blot analysis of Snail1, Twist1, and vimentin proteins of AML cells or AML-chemoresistant cells in each group. (M, N) Representative immunofluorescence images of vimentin and DAPI staining in K562 and K562-ADM cells before and after coculture (red arrow, mesenchymal-like cells; scale bar, 50 μm). $^{*}p < 0.05$, $^{**}p < 0.01$, $^{***}p < 0.001$, $^{****}p < 0.0001$.

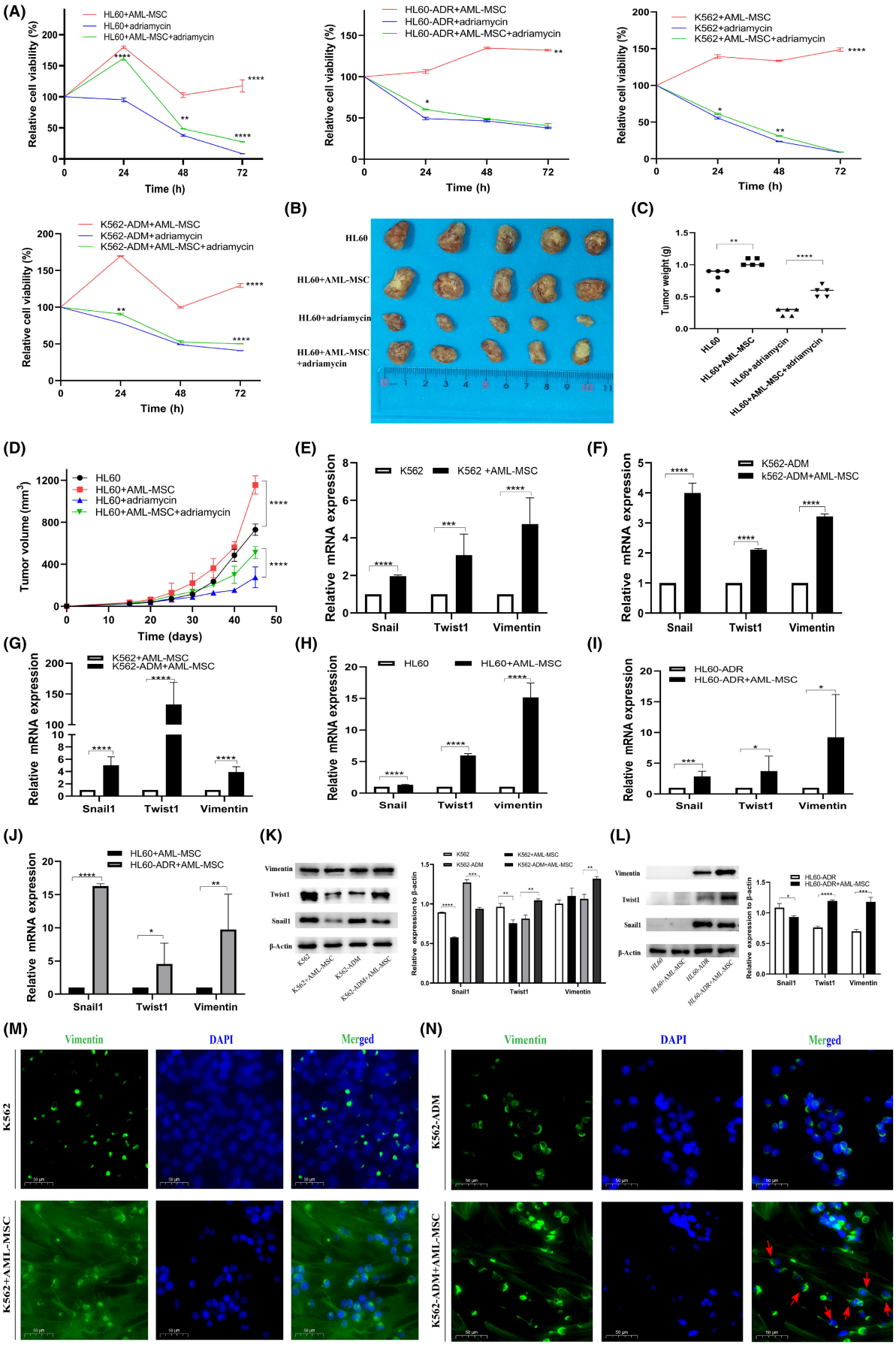
(A)
HL60+AML-MSC
HL60+adriamycin
HL60+AML-MSC+adriamycin
Relative cell viability (%)
Time (h)
HL60-ADR+AML-MSC
HL60-ADR+adriamycin
HL60-ADR+AML-MSC+adriamycin
K562+AML-MSC
K562+adriamycin
K562+AML-MSC+adriamycin
K562-ADM+AML-MSC
K562-ADM+adriamycin
K562-ADM+AML-MSC+adriamycin
(B)
HL60
HL60+AML-MSC
HL60+adriamycin
HL60+AML-MSC +adriamycin
(C)
Tumor weight (g)
HL60
HL60+AML-MSC
HL60+adriamycin
HL60+AML-MSC+adriamycin
(D)
Tumor volume (mm3)
Time (days)
(E)
K562
K562 +AML-MSC
Relative mRNA expression
Snail
Twist1
Vimentin
(F)
K562-ADM
K562-ADM+AML-MSC
(G)
K562+AML-MSC
K562-ADM+AML-MSC
Snail1
(H)
HL60
HL60+AML-MSC
(I)
HL60-ADR
HL60-ADR+AML-MSC
(J)
HL60+AML-MSC
HL60-ADR+AML-MSC
(K)
Vimentin
Twist1
Snail1
β-Actin
Relative expression to β-actin
(L)
(M)
Vimentin
DAPI
Merged
K562
K562+AML-MSC
(N)
K562-ADM
K562-ADM+AML-MSC

analysis was also carried out to assess the EMT-like program. Immunofluorescence staining against vimentin indicated that AML-MSCs induced vimentin cytoskeleton remodeling, several K562-ADM cells in the coculture group showed the spindle morphology with the elongated vimentin cytoskeleton, but this was barely seen in K562 cells (Figure 3M,N).

3.3 | Acute myeloid leukemia MSCs secrete abundant IL-6 into coculture supernatants and upregulate IL-6 expression in AML cells

Mesenchymal stem cells in the tumor microenvironment can activate the EMT profile in tumor cells through its secretions,[25] while

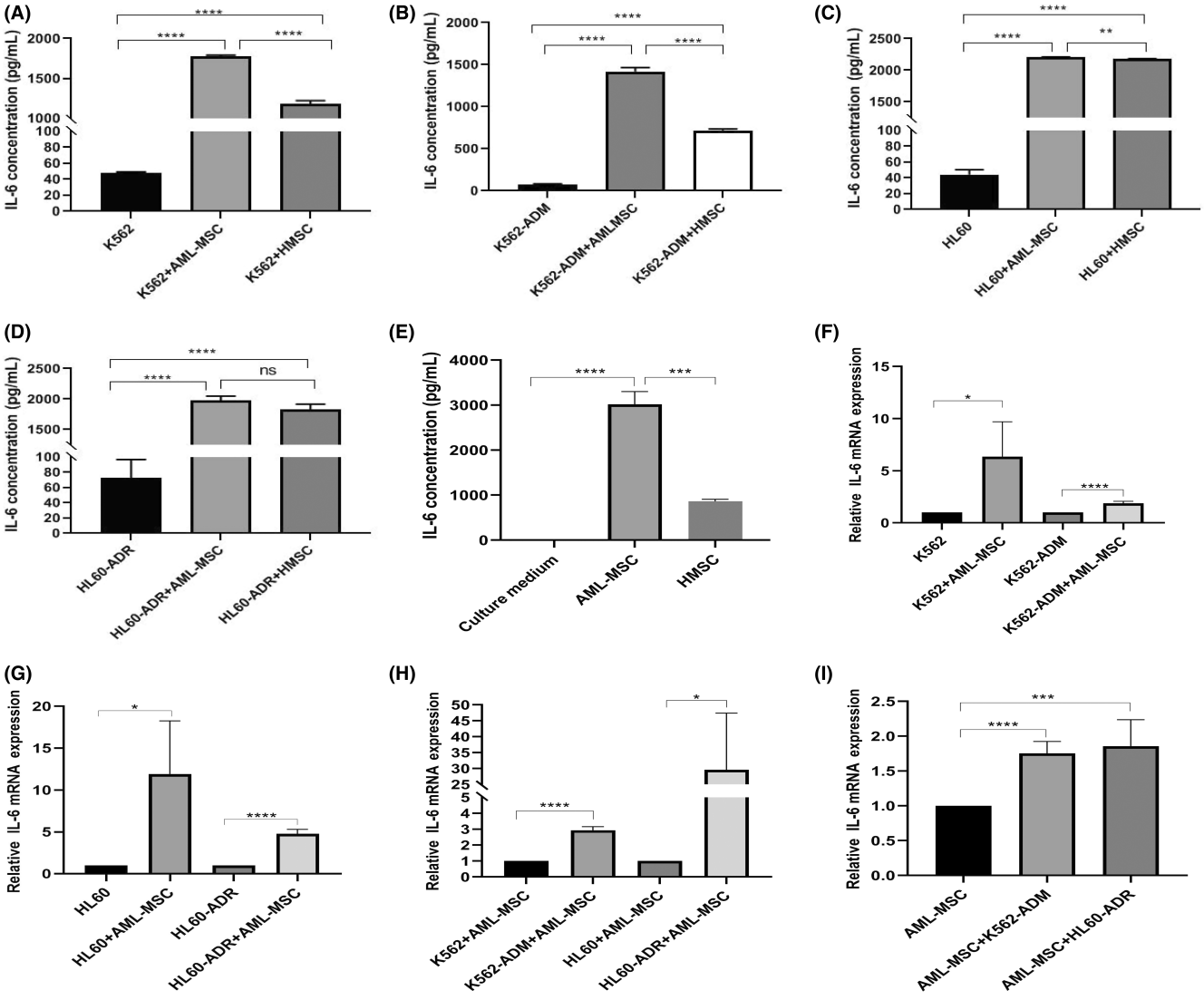

FIGURE 4 Acute myeloid leukemia (AML) bone marrow-derived mesenchymal stem cells (MSCs) secrete abundant interleukin-6 (IL-6) into the coculture supernatants and upregulate IL-6 expression in AML cells. (A–E) IL-6 concentration in supernatants was tested in each group by ELISA. (F–H) IL-6 mRNA expression in K562, adriamycin-resistant K562-ADM, HL60, and adriamycin-resistant HL60-ADR cells was determined by PCR. (I) IL-6 mRNA expression in AML-MSCs was determined by PCR. $^{*}p < 0.01$, $^{**}p < 0.01$, $^{****}p < 0.0001$. HMSC, healthy bone marrow-derived MSC; ns, not significant.

FIGURE 5 Acute myeloid leukemia (AML) bone marrow-derived mesenchymal stem cells (MSCs) promote the epithelial–mesenchymal transition-like process through JAK2/STAT3 signaling in AML cells. (A–C) Jak2 and Stat3 mRNA expression of K562 or adriamycin-resistant K562-ADM cells in each group was determined by PCR. (D–F) Jak2 and Stat3 mRNA expression of HL60 or adriamycin-resistant HL60-ADR cells in each group was determined by PCR. (G) Western blot analysis of Jak2, P-jak2, Stat3, and P-stat3 protein expression in K562 or HL60 cells of each group. (H, I) Western blot analysis of Jak2, P-jak2, Stat3, and P-stat3 and downstream Snail1, Twist1, and vimentin protein expression in K562-ADM and HL60-ADR cells under AG490 treatment. (J, K) Western blot analysis of Jak2, P-jak2, Stat3, and P-stat3 and downstream Snail1, Twist1, and vimentin protein expression in K562-ADM and HL60-ADR cells under ruxolitinib treatment. (L) Interleukin-6 (IL-6) mRNA expression in AML-MSCs was determined by PCR. (M, N) IL-6 concentration in supernatants was tested by ELISA. $^{*}p < 0.05$; $^{**}p < 0.01$; $^{***}p < 0.001$; $^{****}p < 0.0001$. AG490 and ruxolitinib are JAK/STAT pathway inhibitors.

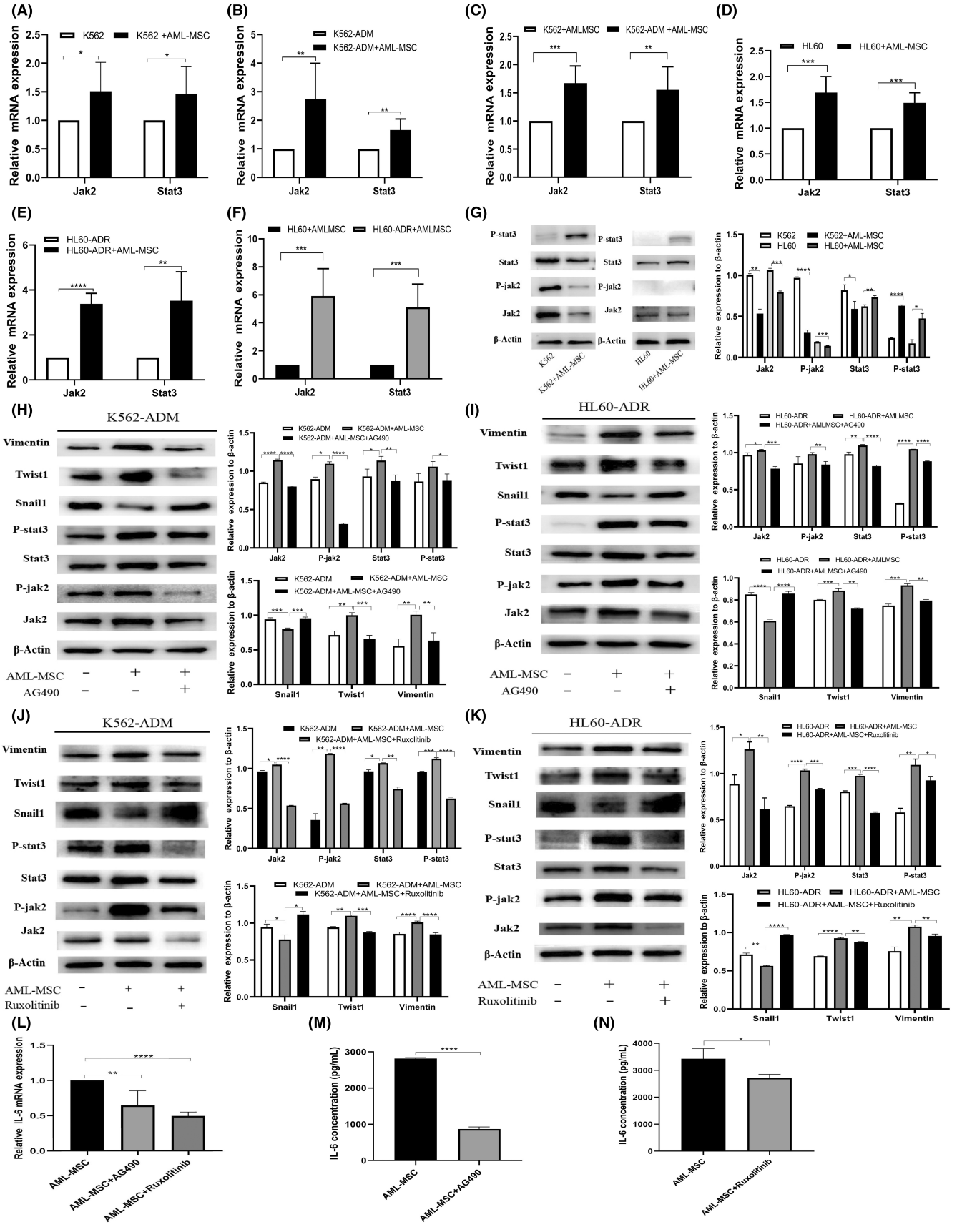

AML-MSCs can secrete abundant IL-6 into the microenvironment.[6] Therefore, we measured the IL-6 levels in the culture supernatants of AML cells alone or coculture systems at 48 h using ELISA. Compared with cultured alone, the IL-6 concentration in the supernatants was significantly higher when AML cells were cocultured with AML-MSCs or HMSCs (Figure 4A–D), AML-MSCs secrete abundant IL-6

and higher than HMSCs (Figure 4E). Furthermore, AML-MSCs upregulated IL-6 expression in AML cells (Figure 4F,G). After coculturing with AML-MSCs, the IL-6 expression in chemoresistant AML cells was higher than their parental cells (Figure 4H). Interestingly, AML cells were in turn upregulated IL-6 expression in AML-MSCs (Figure 4I), activating a positive loop.

3.4 | Acute myeloid leukemia MSCs promote EMT-like process through IL-6/JAK2/STAT3 signaling in AML cells

The IL-6 exerts its action through the JAK/STAT pathway, and the JAK/STAT pathway participates in EMT activation.[26] We speculated that AML-MSC-secreted IL-6 activated the JAK/STAT signaling in AML cells, which contributed to EMT-like change in AML cells. The critical molecules in the JAK/STAT pathway were studied in our experiment. We found that AML-MSCs promoted the relative mRNA expression of Jak2 and Stat3 in K562 and K562-ADM cells (Figure 5A,B). After coculture, K562-ADM cells showed higher Jak2 and Stat3 mRNA expression than K562 cells (Figure 5C). The same result could also be seen in HL60 and HL60-ADR cells (Figure 5D–F). Western blot analysis indicated that AML-MSCs downregulated Jak2 and P-jak2 protein expression in K562 cells and HL60 cells but upregulated the P-Stat3 protein in those two cells (Figure 5G), so AML-MSCs improved the downstream Stat3 activity of the JAK/STAT pathway in K562 cells and HL60 cells. In contrast, AML-MSCs not only promoted the total protein levels but also the phosphorylation of Jak2 and Stat3 in K562-ADM and HL60-ADR cells, so AML-MSCs upregulated the total protein as well as the activity of Jak2 and Stat3 in chemoresistant cells. When AG490 (100 μM), an inhibitor of Jak2, was added to the coculture system for 48 h, it successfully blocked the AML-MSC-induced Jak2/Stat3 signal activation. Moreover, it rescued AML-MSC-induced EMT-related marker expression changes in K562-ADM and HL60-ADR cells (Figure 5H,I). In summary, AML-MSCs can induce the EMT-like program in AML cells through the Jak2/Stat3 pathway. Furthermore, we applied another Jak/Stat pathway inhibitor, ruxolitinib. It inhibited the Jak2/Stat3 pathway and similarly rescued AML-MSC-induced EMT-related marker expression changes in K562-ADM and HL60-ADR cells (Figure 5J,K). Two inhibitors also downregulated IL-6 expression and inhibited IL-6 secretion in AML-MSCs (Figure 5L–N).

3.5 | Inhibitor of JAK2/STAT3 pathway reverses AML-MSC-induced mesenchymal-like morphological change in AML cells

As shown in Figure 5H,I, AG490 reversed AML-MSC-induced EMT marker expression in K562-ADM and HL60-ADR cells. Interestingly, AG490 also reversed the AML-MSC-induced morphological change in K562-ADM and HL60-ADM cells (Figure 6A). The number of mesenchymal-like K562-ADM cells in the cocultured group decreased in the presence of AG490 at 24, 48, and 72 h (all $p < 0.001$; Figure 6B). The number of mesenchymal-like HL60-ADR cells in the cocultured group decreased in the presence of AG490 at 24, 48, and 72 h ($p < 0.05$, $p < 0.001$, and $p < 0.001$, respectively; Figure 6C). Taken together, Jak2/Stat3 pathway inhibitor could reverse the EMT-like change in AML cells.

4 | DISCUSSION

Epithelial–mesenchymal transition is linked to cytoskeleton reorganization and phenotype remodeling in tumor cells, which can change cell–cell and cell–matrix interactions. After EMT, cells acquire an elongated morphology.[27] Epithelial–mesenchymal transition is traditionally restricted to epithelial malignancies, but it cannot be denied that the EMT-like program has been identified in nonepithelial tumors, including leukemia,[28] multiple myeloma,[29] osteosarcoma,[30] and melanoma.[31] In our study, two chemoresistant AML cell lines transformed into a spindle shape from round morphology when AML cells were cocultured with AML-MSCs, which was seldom seen in their parental cells. Healthy bone marrow MSCs also induced mesenchymal-like morphology in chemoresistant cells, but AML-MSCs induced much more mesenchymal-like cells than HMSCs. Meanwhile, AML-MSCs induced expression of EMT markers (Twist1 and vimentin) in AML cells; this effect was more significant in two chemoresistant cells. Acute myeloid leukemia MSCs promoted the mRNA level of Snail1 but inhibited its protein expression; this does not conform to classical EMT regulation. It has been reported that Snail1 protein is unstable and controlled by a specific type of protease.[32] Acute myeloid leukemia MSCs also promoted the mRNA levels of Twist1 and vimentin in K562 cells and HL60 cells, but had the opposite or little effect on relevant protein expressions in K562 cells and HL60 cells, respectively. It had been reported that EMT is dynamic and not a binary process, depending on the cell type and tissue type. Complex aspects orchestrate the EMT, including the pretranscriptional level, transcriptional level, posttranscriptional level, translational level, and posttranslational levels.[33,34] Maybe there were posttranscriptional or posttranslational controls behind the AML-MSC-regulated EMT-like program in AML; this needs to be investigated. Baykal-Köse et al.[35] reported that when leukemia cells were exposed to selective imatinib-mesylate pressure, these cells gained a spindle-like shape. They believed this dynamic and reversible phenotype switch led to therapy resistance in myeloid leukemia. Likewise, we considered this EMT-like phenotype transformation was closely related to chemoresistance progression.

Acute myeloid leukemia has a high rate of treatment failure due to the increased prevalence of therapy resistance; once chemoresistance develops, it is difficult to reverse, contributing to disease relapse and progression. Targeting the AML cells themselves fails to defeat this disease. It is increasingly accepted that the bone marrow microenvironment contributes to AML chemoresistance. Activation of the EMT process in tumors results in

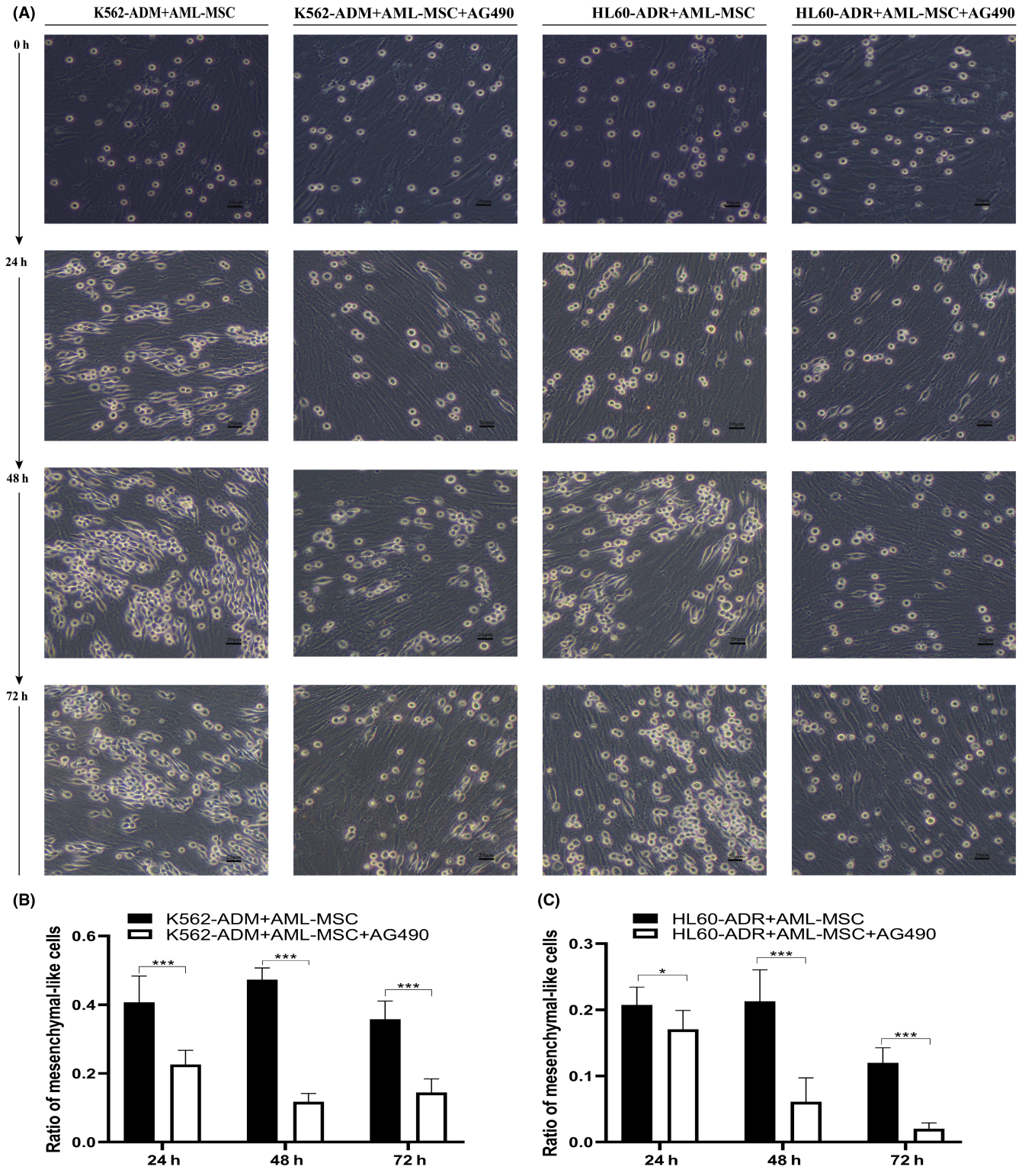

FIGURE 6 Inhibitor of the JAK2/STAT3 pathway reverses acute myeloid leukemia (AML) bone marrow-derived mesenchymal stem cell (MSC)-induced mesenchymal-like morphological change in AML cells. (A) Photomicrographs of adriamycin-resistant K562-ADM and HL60-ADR cells in the AML-MSC coculture system with or without AG490 treatment at 0, 24, 48, and 72 h (magnification, ×100; scale bar, 20 μm). (B) Quantitative analysis of mesenchymal-like K562-ADM cells in two coculture systems at 24, 48, and 72 h. (C) Quantitative analysis of mesenchymal-like HL60-ADR cells in two coculture systems at 24, 48, and 72 h. $^{*}p < 0.05$, $^{***}p < 0.001$.

therapy resistance, and interactions between tumor cells and tumor microenvironment are crucial in multidrug resistance and activation of the EMT.[36] As vital components of the leukemia microenvironment, we found that AML-MSCs promoted AML cell growth and protected AML cells from chemotherapeutic cytotoxicity in vitro and in vivo. Acute myeloid leukemia MSCs also

promoted the proliferation of chemoresistant cells. Lyu et al.[37] reported that HMSCs also promote AML cell proliferation in vitro through their exosomes. On the contrary, Xia et al.[38] found that intra-bone marrow transfusion of HMSCs reduces tumor burden and improves the survival of leukemia-bearing mice. We thought the origin, passages, and numbers of MSCs, as well as the method of coculture might cause different results in tumor growth. In our work, in consideration of the low MSC content in the bone marrow, AML cells and MSCs were cocultured in a 5:1 ratio; we also used AML-MSCs with three to six passages. Therefore, AML-MSCs triggered an EMT-like process in AML cells, particularly in drug-resistant AML cells, which contributed to chemoresistance progression in AML.

We investigated the mechanism behind our findings. In our study, the levels of IL-6 in the AML-MSC or HMSC coculture supernatants were considerably higher than those in the AML alone. The AML-MSCs secreted abundant IL-6 when cultured alone, surpassing the secretion levels of HMSCs; this might be explained by AML-MSCs in the leukemia microenvironment being tumor-associated, and leukemia cells educate them to secrete more cytokines than HMSCs.[39,40] Furthermore, AML-MSCs upregulated the expression of IL-6 in AML, and AML cells in turn promoted the IL-6 expression of AML-MSCs, activating a positive loop that magnifies the IL-6 signaling. It has been reported that MSC secretions recapitulated an EMT-like program in tumor cells.[25] Both Jak2 and Stat3 activation by IL-6 is important for tumor progression in cancer, which can also trigger the EMT process.[41] We found that AML-MSCs contributed to Jak2 and Stat3 activation in AML cells, deeply in drug-resistant cells. To confirm that IL-6/Jak2/Stat3 signaling contributes to the EMT activation in AML, two JAK/STAT pathway inhibitors, AG490 and ruxolitinib, were added to the coculture group. It successfully blocked the Jak2/Stat3 pathway and rescued the AML-MSC-induced EMT marker expression. Furthermore, AG490 reversed the mesenchymal-like morphology change in AML cells of the coculture group. Therefore, when cocultured with AML cells, AML-MSCs secreted considerable IL-6 that activated the Jak2/Stat3 pathway in AML cells; this stimulated the EMT transcription factors that could bind to the vimentin gene's promoter region, upregulating vimentin, resulting in EMT-like change and chemoresistance progression (Figure 7). With the accumulation of reports about the cross-talk between MSCs and tumor cells, the role of MSCs in tumor development is contradictory, and MSC-based cellular therapy in tumors is still controversial.[42,43] However, a large number of studies have reported the pro-tumor effects of IL-6 secreted by MSCs in lung cancer,[15] lymphoma,[44] breast cancer,[45] osteosarcoma,[46] and colorectal cancer.[47] At present, agents targeting IL-6, JAKs, or STATs are in preclinical and clinical investigations; the JAK inhibitor, ruxolitinib has been approved for the treatment of myelofibrosis

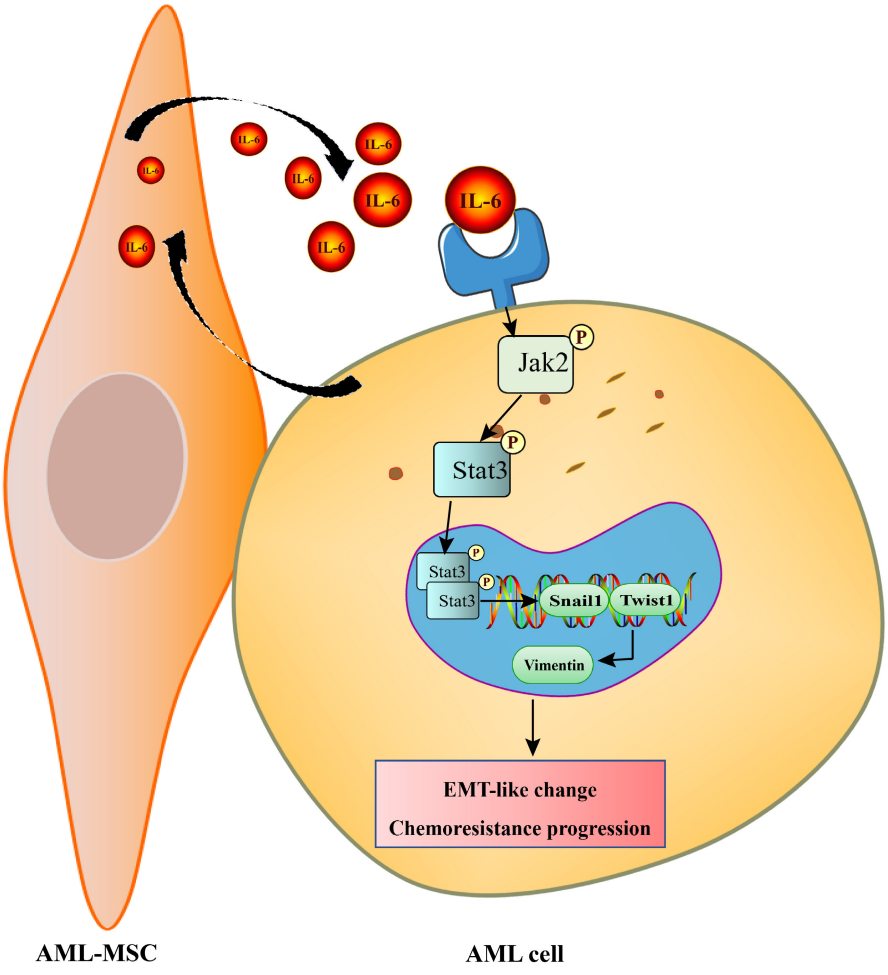

FIGURE 7 Schematic diagram of the mechanism by which acute myeloid leukemia (AML) bone marrow-derived mesenchymal stem cells (MSCs) activate the JAK2/STAT3 pathway in AML cells. The AML-MSCs secrete interleukin-6 (IL-6) and the STAT3 complex enters into the nucleus and leads to transcription of Snail1 and Twist1, which upregulates vimentin, ultimately resulting in epithelial–mesenchymal transition (EMT)-like change and chemoresistance progression in AML cells.

and polycythemia vera.[48] Epithelial–mesenchymal transition has emerged as a therapeutic target for developing novel therapeutic strategies in cancer therapy, and types of anti-EMT drugs are being tested in clinical trials.[49] Our work suggests the potential value of these agents in reversing leukemia microenvironment-mediated chemoresistance progression in AML.

In conclusion, our study shows that AML-MSCs can promote the emergence of chemoresistance in AML cells and accelerate chemoresistance in drug-resistant AML cells. Acute myeloid leukemia MSCs induce the EMT-like characteristics in AML; this phenotypic change could be related to chemoresistance progression. Additionally, AML-MSCs induce the EMT-like program in AML through IL-6/JAK2/STAT3 signaling, which could be a target to reverse chemoresistance in AML.

AUTHOR CONTRIBUTIONS

Jianle Lu and Qiaomei Dong wrote the paper and contributed equally to this study, Jianle Lu conducted the experiments, Qiaomei Dong gave advice in statistical analysis, Shuling Zhang and Youfan Feng gave advice and assistance in phenotypic studies, Jincai Yang participated in review of the manuscript, and Li Zhao and Qiaomei Dong were responsible for design and supervision of experiments.

ACKNOWLEDGMENTS

We thank Dr. Liangliang Li for the assistance in animal experiments.

FUNDING INFORMATION

This work was supported by the Interdisciplinary Project of the First Hospital of Lanzhou University (ldyyyn2020-89), the Fundamental Research Funds of Lanzhou University (lzujbky-2021-kb39), and the Foundation of the First Hospital of Lanzhou University (ldyyyn2020-60, ldyyyn2020-105).

ETHICS STATEMENTS

Approval of the research protocol by an institutional review board: All procedures were authorized by the Institutional Ethics Committee of the First Hospital of Lanzhou University and carried out according to the Declaration of Helsinki.

Informed consent: Written informed consent was obtained from patients or their legal guardians.

Registry and registration no. of the study/trial: N/A.

Animal studies: This study was approved by the Ethics Committee of the First Affiliated Hospital, Lanzhou University.

CONFLICT OF INTEREST STATEMENT

The authors have no conflict of interest.

ORCID

Li Zhao https://orcid.org/0000-0001-5600-5087

REFERENCES

1. Aasebø E, Berven FS, Hovland R, et al. The progression of acute myeloid leukemia from first diagnosis to chemoresistant relapse: a comparison of proteomic and phosphoproteomic profiles. *Cancer*. 2020;12:12.
2. Floren M, Gillette JM. Acute myeloid leukemia: therapy resistance and a potential role for tetraspanin membrane scaffolds. *Int J Biochem Cell Biol*. 2021;137:106029.
3. Forte D, García-Fernández M, Sánchez-Aguilera A, et al. Bone marrow mesenchymal stem cells support acute myeloid leukemia bioenergetics and enhance antioxidant defense and escape from chemotherapy. *Cell Metab*. 2020;32:829-843.e829.
4. Fracchiolla NS, Fattizzo B, Cortelezzi A. Mesenchymal stem cells in myeloid malignancies: a focus on immune escaping and therapeutic implications. *Stem Cells Int*. 2017;2017:6720594.
5. Wang X, Yang Y, Wang N, et al. Mesenchymal stem cell carriers enhance antitumor efficacy induced by oncolytic reovirus in acute myeloid leukemia. *Int Immunopharmacol*. 2021;94:107437.
6. Lopes MR, Pereira JK, de Melo CP, et al. De novo AML exhibits greater microenvironment dysregulation compared to AML with myelodysplasia-related changes. *Sci Rep*. 2017;7:40707.
7. Zhang Y, Guo H, Zhang Z, Lu W, Zhu J, Shi J. IL-6 promotes chemoresistance via upregulating CD36 mediated fatty acids uptake in acute myeloid leukemia. *Exp Cell Res*. 2022;415:113112.
8. Wu J, Zhang L, Feng Y, Khadka B, Fang Z, Liu J. HDAC8 promotes daunorubicin resistance of human acute myeloid leukemia cells via regulation of IL-6 and IL-8. *Biol Chem*. 2021;402:461-468.
9. Dongre A, Weinberg RA. New insights into the mechanisms of epithelial-mesenchymal transition and implications for cancer. *Nat Rev Mol Cell Biol*. 2019;20:69-84.
10. Jiang XM, Xu YL, Yuan LW, et al. TGFβ2-mediated epithelial-mesenchymal transition and NF-κB pathway activation contribute to osimertinib resistance. *Acta Pharmacol Sin*. 2021;42:451-459.
11. Pang X, Zhang J, He X, et al. SPP1 promotes enzalutamide resistance and epithelial-mesenchymal-transition activation in castration-resistant prostate cancer via PI3K/AKT and ERK1/2 pathways. *Oxid Med Cell Longev*. 2021;2021:5806602.
12. Wang B, Ma N, Zheng X, et al. GDF15 repression contributes to 5-fluorouracil resistance in human colon cancer by regulating epithelial-mesenchymal transition and apoptosis. *Biomed Res Int*. 2020;2020:2826010.
13. Gooding AJ, Schiemann WP. Epithelial-mesenchymal transition programs and cancer stem cell phenotypes: mediators of breast cancer therapy resistance. *Mol Cancer Res*. 2020;18:1257-1270.
14. Jiang Y, Han Q, Zhao H, Zhang J. Promotion of epithelial-mesenchymal transformation by hepatocellular carcinoma-educated macrophages through Wnt2b/β-catenin/c-Myc signaling and reprogramming glycolysis. *J Exp Clin Cancer Res*. 2021;40:13.
15. Wang Y, Chu Y, Ren X, et al. Epidural adipose tissue-derived mesenchymal stem cell activation induced by lung cancer cells promotes malignancy and EMT of lung cancer. *Stem Cell Res Ther*. 2019;10:168.
16. Chen SC, Liao TT, Yang MH. Emerging roles of epithelial-mesenchymal transition in hematological malignancies. *J Biomed Sci*. 2018;25:37.
17. Kahlert UD, Joseph JV, Kruyt FAE. EMT- and MET-related processes in nonepithelial tumors: importance for disease progression, prognosis, and therapeutic opportunities. *Mol Oncol*. 2017;11:860-877.
18. Bloehdorn J, Braun A, Taylor-Weiner A, et al. Multi-platform profiling characterizes molecular subgroups and resistance networks in chronic lymphocytic leukemia. *Nat Commun*. 2021;12:5395.
19. Wu SR, Du Y, Beckford J, Alachkar H. Upregulation of the EMT marker vimentin is associated with poor clinical outcome in acute myeloid leukemia. *J Transl Med*. 2018;16:170.
20. Lin J, Zhang W, Niu LT, et al. TRIB3 stabilizes high TWIST1 expression to promote rapid APL progression and ATRA resistance. *Clin Cancer Res*. 2019;25:6228-6242.
21. Gouda MBY, Hassan NM, Kandil EI. Bone marrow overexpression of SNAI1 is an early indicator of intrinsic drug resistance

in patients with de novo acute myeloid leukemia. *J Gene Med*. 2022;25:e3443.
22. Jiang M, He G, Li J, Li J, Guo X, Gao J. Hypoxic exposure activates the B cell-specific Moloney murine leukaemia virus integration site 1/PI3K/Akt axis and promotes EMT in leukaemia stem cells. *Oncol Lett*. 2021;21:98.
23. Liu H, Liu M, Zhang J, Liang Y. Downregulated miR-130a enhances the sensitivity of acute myeloid leukemia cells to Adriamycin. *Mol Med Rep*. 2020;22:2810-2816.
24. Dominici M, Le Blanc K, Mueller I, et al. Minimal criteria for defining multipotent mesenchymal stromal cells. The International Society for Cellular Therapy position statement. *Cytotherapy*. 2006;8:315-317.
25. de Souza LEB, Ferreira FU, Thome CH, et al. Human and mouse melanoma cells recapitulate an EMT-like program in response to mesenchymal stromal cells secretome. *Cancer Lett*. 2021;501:114-123.
26. Abaurrea A, Araujo AM, Caffarel MM. The role of the IL-6 cytokine family in epithelial-mesenchymal plasticity in cancer progression. *Int J Mol Sci*. 2021;22:22.
27. Leggett SE, Hruska AM, Guo M, Wong IY. The epithelial-mesenchymal transition and the cytoskeleton in bioengineered systems. *Cell Commun Signal*. 2021;19:32.
28. Chirillo R, Aversa I, Di Vito A, et al. FtH-mediated ROS dysregulation promotes CXCL12/CXCR4 Axis activation and EMT-like trans-differentiation in erythroleukemia K562 cells. *Front Oncol*. 2020;10:698.
29. Peng Y, Li F, Zhang P, et al. IGF-1 promotes multiple myeloma progression through PI3K/Akt-mediated epithelial-mesenchymal transition. *Life Sci*. 2020;249:117503.
30. Bi W, Yang M, Xing P, Huang T. MicroRNA miR-331-3p suppresses osteosarcoma progression via the Bcl-2/Bax and Wnt/β-catenin signaling pathways and the epithelial-mesenchymal transition by targeting N-acetylglucosaminyltransferase I (MGAT1). *Bioengineered*. 2022;13:14159-14174.
31. Wei CY, Zhu MX, Yang YW, et al. Downregulation of RNF128 activates Wnt/β-catenin signaling to induce cellular EMT and stemness via CD44 and CTTN ubiquitination in melanoma. *J Hematol Oncol*. 2019;12:21.
32. Lambies G, García de Herreros A, Díaz VM. The role of DUBs in the post-translational control of cell migration. *Essays Biochem*. 2019;63:579-594.
33. Bakir B, Chiarella AM, Pitarresi JR, Rustgi AK. EMT, MET, plasticity, and tumor metastasis. *Trends Cell Biol*. 2020;30:764-776.
34. Li D, Xia L, Huang P, et al. Heterogeneity and plasticity of epithelial-mesenchymal transition (EMT) in cancer metastasis: focusing on partial EMT and regulatory mechanisms. *Cell Prolif*. 2023;e13423.
35. Baykal-Köse S, Acikgoz E, Yavuz AS, et al. Adaptive phenotypic modulations lead to therapy resistance in chronic myeloid leukemia cells. *PLoS One*. 2020;15:e0229104.
36. Erin N, Grahovac J, Brozovic A, Efferth T. Tumor microenvironment and epithelial mesenchymal transition as targets to overcome tumor multidrug resistance. *Drug Resist Updat*. 2020;53:100715.
37. Lyu T, Wang Y, Li D, et al. Exosomes from BM-MSCs promote acute myeloid leukemia cell proliferation, invasion and chemoresistance via upregulation of S100A4. *Exp Hematol Oncol*. 2021;10:24.
38. Xia C, Wang T, Cheng H, et al. Mesenchymal stem cells suppress leukemia via macrophage-mediated functional restoration of bone marrow microenvironment. *Leukemia*. 2020;34:2375-2383.
39. Borella G, Da Ros A, Borile G, et al. Targeting the plasticity of mesenchymal stromal cells to reroute the course of acute myeloid leukemia. *Blood*. 2021;138:557-570.
40. Frisbie L, Buckanovich RJ, Coffman L. Carcinoma-associated mesenchymal stem/stromal cells: architects of the pro-tumorigenic tumor microenvironment. *Stem Cells*. 2022;40:705-715.
41. Manore SG, Doheny DL, Wong GL, Lo HW. IL-6/JAK/STAT3 signaling in breast cancer metastasis: biology and treatment. *Front Oncol*. 2022;12:866014.
42. Liang W, Chen X, Zhang S, et al. Mesenchymal stem cells as a double-edged sword in tumor growth: focusing on MSC-derived cytokines. *Cell Mol Biol Lett*. 2021;26:3.
43. Klopp AH, Gupta A, Spaeth E, Andreeff M, Marini F 3rd. Concise review: dissecting a discrepancy in the literature: do mesenchymal stem cells support or suppress tumor growth? *Stem Cells*. 2011;29:11-19.
44. Zhong W, Zhu Z, Xu X, et al. Human bone marrow-derived mesenchymal stem cells promote the growth and drug-resistance of diffuse large B-cell lymphoma by secreting IL-6 and elevating IL-17A levels. *J Exp Clin Cancer Res*. 2019;38:73.
45. Xu H, Zhou Y, Li W, et al. Tumor-derived mesenchymal-stem-cell-secreted IL-6 enhances resistance to cisplatin via the STAT3 pathway in breast cancer. *Oncol Lett*. 2018;15:9142-9150.
46. Lu M, Xie K, Lu X, Lu L, Shi Y, Tang Y. Notoginsenoside R1 counteracts mesenchymal stem cell-evoked oncogenesis and doxorubicin resistance in osteosarcoma cells by blocking IL-6 secretion-induced JAK2/STAT3 signaling. *Invest New Drugs*. 2021;39:416-425.
47. Zhang X, Hu F, Li G, et al. Human colorectal cancer-derived mesenchymal stem cells promote colorectal cancer progression through IL-6/JAK2/STAT3 signaling. *Cell Death Dis*. 2018;9:25.
48. Johnson DE, O'Keefe RA, Grandis JR. Targeting the IL-6/JAK/STAT3 signalling axis in cancer. *Nat Rev Clin Oncol*. 2018;15:234-248.
49. Jonckheere S, Adams J, De Groote D, Campbell K, Berx G, Goossens S. Epithelial-mesenchymal transition (EMT) as a therapeutic target. *Cells Tissues Organs*. 2022;211:157-182.

SUPPORTING INFORMATION

Additional supporting information can be found online in the Supporting Information section at the end of this article.

How to cite this article: Lu J, Dong Q, Zhang S, Feng Y, Yang J, Zhao L. Acute myeloid leukemia (AML)-derived mesenchymal stem cells induce chemoresistance and epithelial–mesenchymal transition-like program in AML through IL-6/JAK2/STAT3 signaling. *Cancer Sci*. 2023;114:3287-3300. doi:10.1111/cas.15855